Contrasting ambient fine particles hygroscopicity derived by HTDMA and HR-AMS measurements between summer and winter in urban Beijing

Xinxin Fan[1], Jieyao Liu[1], Fang Zhang[1*], Lu Chen[1], Don Collins[2], Weiqi Xu[3, 4], Xiaoai Jin[1], Jingye Ren[1],Yuying Wang[1, 5], Hao Wu[1], Shangze Li[1], Yele Sun[3, 4], Zhanqing Li[1, 6]

[1]*State Key Laboratory of Earth Surface Processes and Resource Ecology, College of Global Change and Earth System Science, Beijing Normal University, Beijing 100875, China*
[2]*Department of Chemical and Environmental Engineering, University of California Riverside, Riverside, California, USA*
[3]*State Key Laboratory of Atmospheric Boundary Layer Physics and Atmospheric Chemistry, Institute of Atmospheric Physics, Chinese Academy of Sciences, Beijing 100029, China*
[4] *College of Earth Sciences, University of Chinese Academy of Sciences, Beijing 100049, China*
[5]*School of Atmospheric Physics, Nanjing University of Information Science and Technology, Nanjing 210044, China*
[6]*Earth System Science Interdisciplinary Center and Department of Atmospheric and Oceanic Science, University of Maryland, College Park, Maryland, USA*

Correspondence to: Fang.zhang@bnu.edu.cn

Abstract

The effects of aerosols on visibility through scattering and absorption of light and on climate through altering cloud droplet concentration are closely associated with their hygroscopic properties. Here, based on field campaigns in winter and summer in Beijing, we compare the size-resolved hygroscopic parameter (κ_{gf}) of ambient fine particles derived by an HTDMA (Hygroscopic Tandem Differential Mobility Analyzer) to that (denoted as κ_{chem}) of calculated by an HR-ToF-AMS (High-resolution Time-of-Flight Aerosol Mass Spectrometer) measurements using a simple rule with a uniform internal mixing hypothesis. We mainly focus on contrasting the disparity of κ_{gf} and κ_{chem} between summer and winter to reveal the impact of atmospheric processes/sources on aerosols hygroscopicity and to evaluate the uncertainty in estimating particles hygroscopicity with the hypothesis. We show that, in summer, the κ_{chem} for 110, 150 and 200 nm particles was averagely ~10% - 12% lower than κ_{gf}, with the greatest difference between the values observed around noontime when aerosols experience rapid photochemical aging. In winter, no apparent disparity between κ_{chem} and κ_{gf} is observed for those >100 nm particles around noontime, but the κ_{chem} is much higher than κ_{gf} in the late afternoon when ambient aerosols are greatly influenced by local traffic and cooking

sources. By comparing with the observation from other two sites (Xingtai, Hebei and Xinzhou, Shanxi) of north China, we verify that atmospheric photochemical aging of aerosols enhances their hygroscopicity and may induce a coating effect which thereby leads to 10%-20% underestimation of the hygroscopic parameter if using the uniform internal mixing assumption. The coating effect is found more significant for these >100 nm particles observed in remote or clean regions. However, local primary sources, which result in a large number of externally-mixed BC and POA (Primary Organic Aerosol) in urban Beijing during traffic rush hour time, cause 20-40% overestimation of the hygroscopic parameter. This is largely due to an inappropriate use of density of the BC that is closely associated with its morphology, and the results show that the calculation can be improved by applying an effective density of freshly BC within the range of 0.25-0.45 g cm^{-3} in the mixing rule assumption. Our study suggest that it is critical to measure the effective density and morphology of ambient BC in particularity in those regions with complex local sources, so as to accurately parameterize the effect of BC aging on particles hygroscopicity.

1. Introduction

The effects of aerosols on visibility through scattering and absorption of light and on climate through altering cloud droplet concentration are influenced by their hygroscopic growth. Understanding and reducing the uncertainty in prediction of the aerosol hygroscopic parameter (κ) using chemical composition would improve model predictions of aerosol effects on clouds and climate.

The hygroscopic properties of both the natural and anthropogenic aerosols, in addition to being affected by its chemical composition (Gunthe et al., 2009), are also affected by the particle mixing state and aging (Schill et al., 2015; Peng et al., 2017). For example, a recent laboratory study shown that the coexisting hygroscopic species have a strong influence on the phase state of particles, thus affecting chemical interactions between inorganic and organic compounds as well as the overall hygroscopicity of mixed particles (Peng et al., 2016). The field measurements also demonstrated that the hydrophobic black carbon particles became hygroscopic with atmospheric mixing and aging by organics (i.e. Peng et al., 2017). In a heavily polluted atmosphere, the aerosol sources and sinks are varied, the physical and chemical processes experienced by the aerosols are complex, and the mixing state and its impact on aerosols hygroscopicity is

more complicated. The hygroscopicity of mixed particles and mutual impacts between the components are still poorly understood.

Previous studies have shown that the difference between the κ obtained from H-TDMA or CCNc measurements and that calculated based on the volume mixing ratio of chemical components, κ_{chem}. Laboratory results from Cruz and Pandis (2000) indicate that κ_{gf} of internally mixed ammonium sulfate and organic matter is higher than κ_{chem} calculated for assumed uniform internal mixing. But Peng et al (2016) found that, for sodium chloride and organic aerosols mixed particles, the measured growth factors by H-TDMA were significantly lower than calculations from the mixing rule methods. In some field studies on aged aerosols, the κ was underestimated by the calculation based on uniform internal mixing assumption and thus lead to an underestimation of CCN concentration(Bougiatioti, et al., 2009; Chang, et al., 2007; Kuwata, et al., 2008; Wang, et al., 2010; Ren et al., 2018). However, for primary emissions dominated periods, the κ value from calculations based on bulk chemical composition was much higher than that measured by H-TDMA measurements (Zhang et al., 2017). The various results from previous studies suggest distinct effects of aerosols mixing state on their hygroscopicity. Overall, to what extent do the differences depend on the mixing state and the extent of aging of the particles, and how the different atmospheric processes and what kinds of mixing structure of the particles may result in those disparity between measured and calculated hygroscopic parameter have not been clearly clarified by the previous studies. A comprehensive and systematic investigation on the cause and magnitude of the effect has been lacking.

In the atmosphere, the κ, which is related to the particle mixing state diversity, varies largely across the size range of ambient fine particles (Rose et al., 2010). Previous study only compared the measured κ to that calculated based on bulk chemical composition (Zhang et al., 2017). Using size-resolved, not bulk, chemical composition measurements in different seasons is expected to provide more comprehensive understanding and insights of how the aerosols mixing state influence on their hygroscopicity, motivating our analysis that employs size-resolved chemical composition measured by an HR-ToF-AMS in this study. The aim of this paper is to study the hygroscopicity and mixing state characteristics of fine particles in the Beijing urban area, and to reveal the impact of atmospheric processes/sources and mixing/aging on aerosols

hygroscopicity and elucidate the uncertainty in calculating the hygroscopic parameter using simple mixing rule estimates based on size-resolved chemical composition. The experiment and theory in the study are introduced in Sect. 2. The comparison between the hygroscopic parameter obtained from the HTDMA and and that calculated using size-resolved chemical composition is discussed in Sect. 3. Conclusions from the study are given in Sect. 4.

2. Experiment and Theory

2.1. Site and instruments

Two field campaigns are conducted during winter 2016 and summer 2017 of urban Beijing (Fig. 1, BJ: 39.97 °N, 116.37 °E) for measurements of aerosols physical and chemical properties. The BJ site is located at the Institute of Atmospheric Physics (IAP), Chinese Academy of Sciences, which is between the north third and fourth ring roads in northern Beijing. Local traffic and cooking emissions can be important at the site (Sun et al., 2015). The sampling period in cold season was from 16 November to 10 December 2016, during the domestic heating period in Beijing. The sampling period in warm season was from 25 May to 18 June 2017.

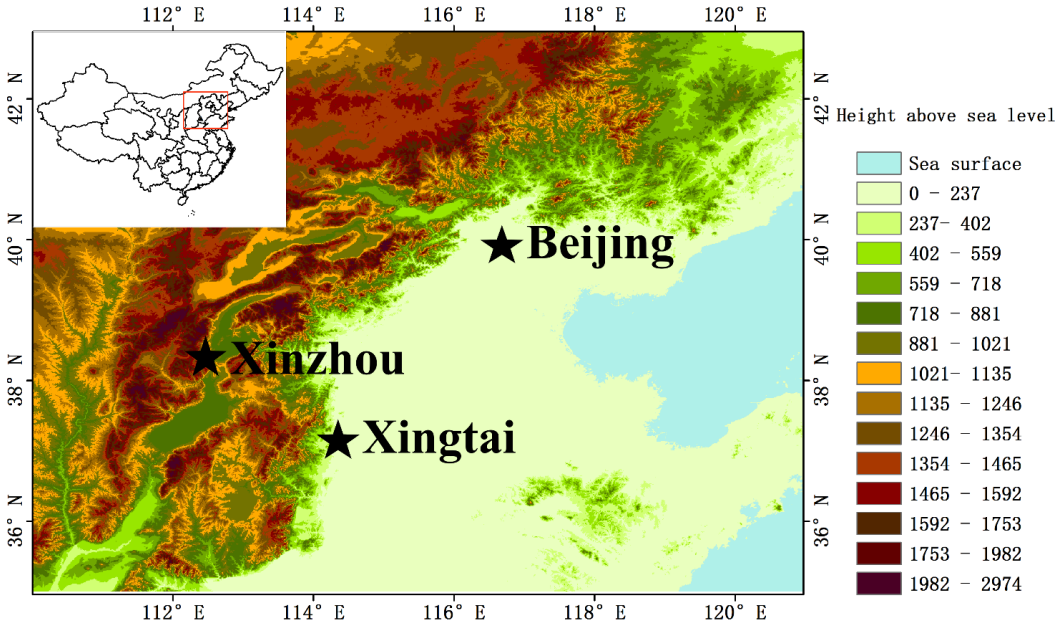

Figure 1. The map location of the sites

Particle number size distribution (PNSD) in the size range from 10 nm to 550 nm was measured with a Scanning Mobility Particle Sizer (SMPS; Wang & Flagan, 1990; Collins et al., 2002), which consists of a long differential mobility analyzer (DMA, model 3081L, TSI Inc) to classify the particle and a condensation particle counter (CPC, model 3772, TSI Inc.) to detect the size classified particles. The sampled particles were dried to relative humidity < 30% before entering the DMA. The measurement time for each size distribution was five minutes.

The HTDMA system used in this study has been described in detail in previous publications (Tan et al., 2013; Wang et al., 2017; Zhang et al., 2017). Here, only a brief description is given. A Nafion dryer dried the sampled particles to relative humidity < 20%, after which the steady state charge distribution was reached in a bipolar neutralizer. The first differential mobility analyzer (DMA_1, model 3081L, TSI Inc.) selected the quasi-monodisperse particles through applying a fixed voltage. The dry diameters selected in this study were 40, 80, 110, 150, and 200 nm. The quasi-monodisperse particles were humidified to a controlled RH (90% in this study) using a Nafion humidifier. A second DMA (DMA_2, same model as the DMA_1) coupled with a water-based condensation particle counter (WCPC, model 3787, TSI Inc.) measured the particle number size distributions of the humidified aerosol. RH calibration with ammonium sulfate was carried out regularly during the study.

The hygroscopic growth factor (Gf) is defined as the ratio of the mobility diameter at a given RH to the dry diameter:

$$\mathrm{Gf} = \frac{D(RH)}{D(dry)}$$

The Gf probability density function (PDF) is retrieved based on the $TDMA_{inv}$ algorithm developed by Gysel et al. (2009). Dry scans in which the RH between the two DMAs was not increased were used to define the width of the transfer function.

Size-resolved non-refractory submicron aerosol composition was measured with an Aerodyne high-resolution time-of-flight aerosol mass spectrometer (HR-ToF-AMS; Xu et al., 2015). The particle mobility diameter was estimated by dividing the vacuum aerodynamic diameter from the AMS

measurements by particle density. Because the uncertainty caused by the fixed density across the size range is negligible (Wang et al. 2016), here, the particle density is assumed to be 1600 kg m^{-3} (Hu et al., 2012). AMS positive matrix factorization (PMF) with the PMF2.exe (v4.2) method was performed to identify various factors of organic aerosols. Xu et al. (2015) have described the operation and calibration of the HR-ToF-AMS in detail. Black carbon (BC) mass concentration was derived from measurements of light absorption with a 7-wavelength aethalometer (AE33, Magee Scientific Corp.; Zhao et al., 2017).

2.2. Data

The time series of the submicron particle mass concentration PM_1, bulk mass concentrations of the main species in PM_1, mass fraction of the chemical composition of PM_1, and probability density function of growth factor (Gf-PDFs) for 40 and 150 nm particles during the campaign are presented in Fig. 2. Quite distinct temporal variability of aerosol chemical and physical properties was observed between winter and summer. The average mass concentration of PM_1 was 55.2 μg/m^3 in the winter and 16.5 μg/m^3 in the summer during our study periods. In this study, we define the conditions when the mass concentration in winter period was < 20 μg m^{-3} and >80 μg m^{-3} as clean and polluted conditions, respectively. Organic aerosol (OA), consisting of secondary organic aerosol (SOA) and primary organic aerosol (POA), was the major fraction during both the winter and summer sampling periods. POA concentration was higher than that of SOA in the winter, which reflects the influence of primary emissions such as coal combustion OA (COOA) in Beijing (Hu et al., 2016; Sun et al., 2016). In contrast, SOA usually dominated in the summer, which is evident that secondary aerosol formation played a key role in the source of PM_1. Distinct hydrophobic (with Gf of ~1.0) and more hygroscopic (with Gf of ~1.5) modes were observed from Gf-PDFs of both small and large particles. Sometimes the more hygroscopic mode particles were more concentrated and at others the hydrophobic particles were. In general though, the more hygroscopic mode dominated for larger particles (i.e. 150 nm), and the less hygroscopic mode did for the smallest particles (e.g. 40 nm). Occasionally, only the hydrophobic mode was evident for 150 nm particles, which occurred when POA dominated the PM_1. Only the hygroscopic mode was discernable for 40 nm particles during new particle formation (NPF) events that occurred more frequently in summer than winter (Fig. 3).

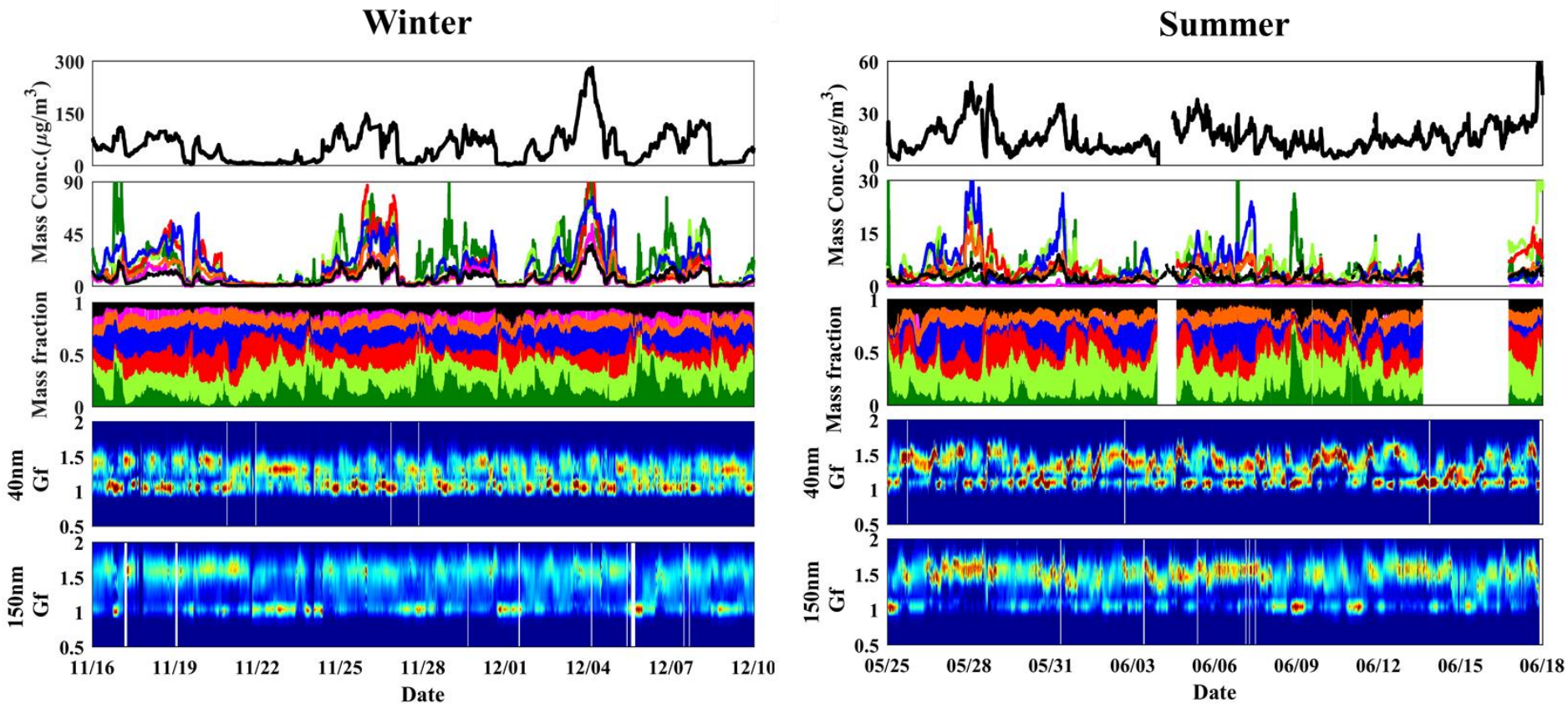

Figure 2. Winter (left) and summer (right) time series of mass concentration of PM_1, bulk mass concentration of the main species in PM_1, mass fraction of the chemical composition of $PM_1$and Gf-PDFs for 40 and 150 nm particles.

2.3. Theory and method

2.3.1 Derivation of the hygroscopic parameter, κ, from the growth factor (Gf)

According to κ -Köhler Theory (Petters and Kreidenweis, 2007), the hygroscopicity parameter κ can be derived using the growth factor measured by an HTDMA.

$$\kappa = (Gf^3 - 1)\left(\frac{\exp\left(\frac{A}{D_d Gf}\right)}{RH} - 1\right) \quad , \tag{1}$$

$$\mathrm{A} = \frac{4\sigma_{s/a} M_w}{RT\rho_w} \quad , \tag{2}$$

where Gf is hygroscopic growth factor measured by HTDMA, D_d is the dry diameter of the particles, RH is the relative humidity in the HTDMA (90%, in our study), $\sigma_{s/a}$ is the surface tension of the solution/air (assumed here to be the surface tension of pure water, $\sigma_{s/a}$ = 0.0728 N m^{-2}), M_w is the molecular weight of water, R is the universal gas constant, T is the absolute temperature, and ρ_w is the density of water.

2.3.2 Derivation of the hygroscopic parameter, κ, from chemical composition data

For an assumed internal mixture, κ can also be calculated by a simple mixing rule on the basis of chemical volume fractions (Petters and Kreidenweis, 2007; Gunthe et al., 2009):

$$\kappa_{chem} = \sum_i \varepsilon_i \kappa_i \quad , \tag{3}$$

where κ_i and ε_i are the hygroscopicity parameter and volume fraction for the individual (dry) component in the mixture, respectively. The AMS provides mass concentrations of organics and of many inorganic ions. The inorganic components mainly consisted of $(NH_4)_2SO_4$ and NH_4NO_3 (Zhang et al., 2014). And the values of κ are 0.48 for $(NH_4)_2SO_4$ and 0.58 for NH_4NO_3 (Petters and Kreidenweis, 2007). To estimate κ_{org}, we used the following linear function derived by Mei et al. (2013): κ_{org} = 2.10 × f_{44} – 0.11. We derived the volume fraction of each species by dividing mass concentration by its density. The density are 1.77 g cm^{-3}

for $(NH_4)_2SO_4$ and 1.72 g cm^{-3} for NH_4NO_3. The densities of organics are assumed to be 1.2 g cm^{-3} (Turpin et al., 2001). The κ and density of BC are assumed to be 0 and 1.7 g cm^{-3}. In the following discussions, κ_{gf} and κ_{chem} denote the values derived from HTDMA measurements and calculated using the ZSR mixing rule, respectively.

In addition, we also compare the results from the field campaigns with those from other two sites, Xingtai (XT: 37.18 °N，114.37 °E), and Xinzhou (XZ: 38.24 °N，112.43 °E), in North China Plain (Fig. 1). At XZ site, we use the hygroscopic parameter (defined as κ_{CCNc}) from size-resolved CCN measurements (Zhang et al., 2014, 2016) for comparison. More detailed descriptions of the method to retrieve κ_{CCNc} can be found in (Petters and Kreidenweis (2007). Both of the κ_{gf} and κ_{CCNc} are derived based on κ -Köhler Theory (Petters and Kreidenweis, 2007). But, different from the κ_{gf} measured by the HTDMA system which is operated at RH of 90%, the κ_{CCNc} is derived by measuring aerosols CCN activity under the condition of supersaturations with relative humidity of >100%. Previous studies from filed measurements and laboratory experiments showed that the κ_{CCNc} is generally slight larger or smaller than κ_{gf}, but they are basically comparable and can well represent an overall aerosols hygroscopisity (e.g. Carrico et al., 2008; Wex et al., 2009; Good et al., 2010; Irwin et al., 2010; Cerully et al., 2011; Wu et al., 2013; Zhang et al., 2017).

3. Results and discussion

3.1. Diurnal variations of ambient fine particles physiochemical properties and hygroscopic growth factor

The diurnal variations of the PNSD, mass concentration of PM_1, mass concentration and fraction of chemical components in PM_1, and Gf-PDFs for 40 and 150 nm particles during the campaign are shown in Fig. 3. During the summer an obvious peak value in the PNSD is observed around noontime due to NPF events that typically started around 10:00 LT (Local Time). The resulting sharp increase in number concentration of nucleation mode particles was followed by decreased concentration and a rapid growth in diameter of the particles along with increased mass concentration of SOA and sulfate in PM_1, indicating

strong photochemical and secondary formation processes during daytime in the summer (Marked in red box in Fig. 3). In contrast, NPF was not evident during the winter period, which may in part be due to the much higher (~3x) PM_1 mass concentrations in the winter than in the summer. Note that peak values in number concentration and in mass concentrations of PM_1 and POA occurred during the early evening (17:00-21:00, LT) indicating the strong impact of local sources from traffic emissions and cooking (Marked in black box in Fig. 3). In addition, the diurnal cycles of aerosol physical and chemical properties are also influenced by the diurnal changes in the planetary boundary layer (PBL) that leads to accumulation of particles during nighttime when higher values of both number and mass concentration were observed.

Owing to the continued local and primary emissions near the study site, the Gf-PDFs for 40 nm particles generally display a bimodal shape with more and less hygroscopic modes (with Gf of ~ 1.5 and ~ 1.1 respectively) throughout the day both in winter and summer periods, indicating an external mixing state for the 40 nm particles. Note that, during nighttime and early morning in the winter, the more hygroscopic mode dominated and was shifted to higher Gf than during the daytime. This is thought to be due to heterogeneous/aqueous reactions on pre-existing primary small particles, and/or coagulation/condensation processes that are enhanced at night under lower ambient temperature and higher relative humidity, all of which result in a more hygroscopic and more internally-mixed aerosol (Liu et al., 2011; Massling et al., 2005; Ye et al., 2013; Wu et al., 2016; Wang et al., 2018a).). Interestingly, in the summer period, the concentration of the hydrophilic mode increased quickly around noontime and in the early afternoon (12:00-16:00), with a corresponding decrease in the relative concentration of the hydrophobic mode, which likely indicates a transformation of the particles from externally to internally mixing state as a result of the species condensation from the photochemical reaction (Wu et al., 2016; Wang et al., 2017), resulting in an increase in particle hygroscopicity. In addition, it is evident that 40 nm particles after 12:00 were dominated by NPF (Fig. 3). Therefore, the increase of hydrophobic mode particles suggests that a large amount of hydrophilic particles are generated from NPF. For 150 nm particles, the hygroscopic mode in the Gf-PDF is more dominant during daytime in particular during the summer period when the strong solar radiation promotes photochemical aging and growth, thus producing a more internally-mixed aerosol. The dominant

hydrophobic mode at around 18:00 was observed both in winter and summer and reflects abundant traffic emissions and cooking sources (primarily with POA) during the early evening period.

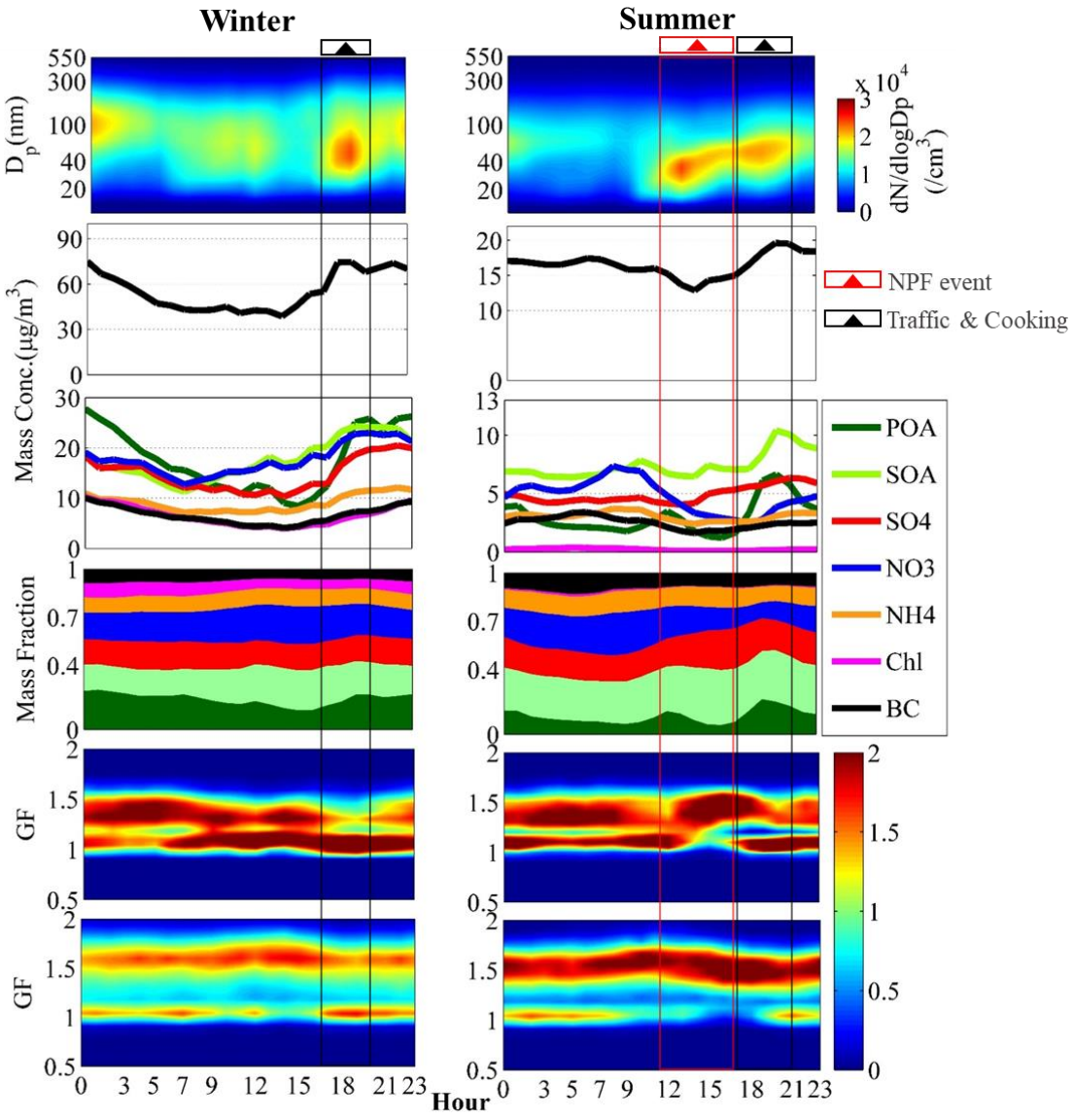

Figure 3. Campaign averaged diurnal variations in particle number size distribution; mass concentration of PM_1, bulk mass concentration of main species in PM_1, mass fraction of chemical composition of PM_1; and Gf-PDFs for 40 and 150 nm particles in winter (left panels) and summer (right panels) measured in urban Beijing..

3.2 κ_{gf} dependence on D_p

The size dependence of particle hygroscopicity parameters for the winter and summer periods are presented in Fig.4. In the winter, the 40 nm particles were least hygroscopic and the hygroscopicity of larger

particles (>80 nm) displayed insignificant dependence on particle size. The size independence for the larger particles is consistent with the observed similarity in mass fractions of inorganic and organic species across

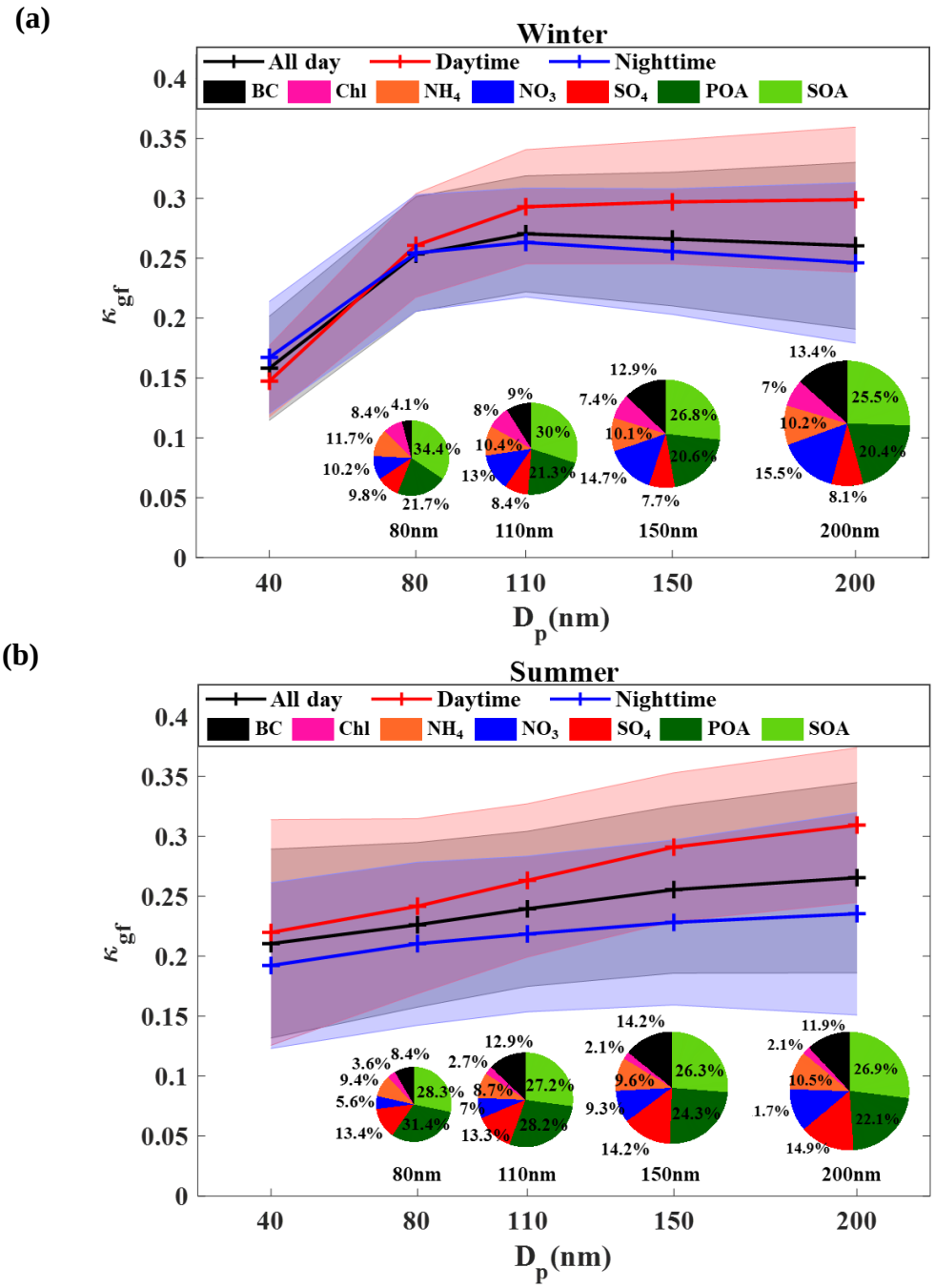

Figure 4. The dependence of κ on D_p at the urban Beijing site during winter (a) and summer (b). The κ values are retrieved from the size-resolved HTDMA measurements. The error bars represent $\pm 1\sigma$. The size-resolved chemical mass fractions at the corresponding D_p is also presented.

the size range as shown in the pie charts in Figure 4a. A similar dependence of particle hygroscopicity on particle size was also observed in the urban area of Beijing during the wintertime of 2014 (Wang et al.,

2018b). In the summer, hygroscopicity increased with increasing particle size, which is expected based on the size dependent patterns shown in the pie charts, with the mass fraction of POA decreasing with the particles size and the mass fraction of inorganics like sulfate and nitrate increasing with particle size.

3.3. Closure of HTDMA and chemical composition derived κ

A closure study was conducted between κ_{chem} and κ_{gf} (Fig. 5) to investigate the uncertainty of the two methods, and especially to further illustrate whether particle hygroscopicity can be well predicted by κ_{chem} calculated by assuming internal mixing. Since a size-resolved BC mass concentration measurement was not

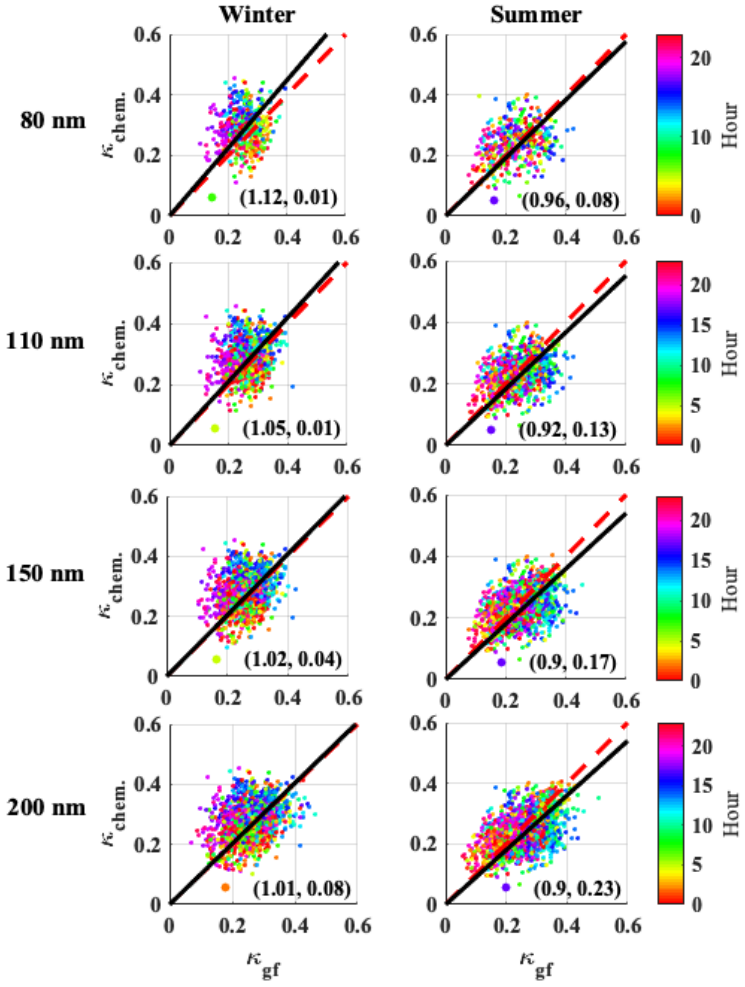

Figure 5. Closure of κ_{chem} calculated from size-resolved chemical composition data and κ_{gf} retrieved from hygroscopic growth factor by HTDMA measurements in winter (left panels) and summer (right panels) period. The dots with different color correspond to observed time of a day during the campaign as shown by the color bar. On each plot, red dotted line is 1:1 line, black solid line is fitting line. The numbers in parentheses are slopes of linear fits and correlation coefficients (R^2).

available during the campaign, we use the bulk mass fraction of BC particles measured by the AE33 combining with size-resolved BC distribution measured by a single particle soot photometer (SP2) in Beijing (Liu et al., 2018) to estimate κ_{chem}. During the calculation, the BC core diameter measured by SP2 has been converted to the diameter of coated BC particles by multiplying factors of 1.4 and 2.6 under clean (with bulk BC mass concentrations <2 μg m^{-3}) and polluted (with bulk BC mass concentrations >2 μg m^{-3}) conditions respectively (Liu et al., 2018).

Uncertainty in κ is due in part to measurement uncertainty of the HTDMA system and uncertainty resulting from non-ideality effects in the solution droplets, surface tension reduction due to surface active substances, and the presence of slightly soluble substances that dissolve at RH higher than that maintained in the HTDMA (e.g., Wex et al., 2009; Good et al., 2010; Irwin et al., 2010; Cerully et al., 2011; Wu et al., 2013). However, our previous study demonstrated that, for this region, estimates using HTDMA data are still better representing the aerosols hygroscopicity than those using the simple mixing rule based on chemical volume fractions for an assumed internal mixture (Zhang et al., 2017). Therefore, here we focus on discussing and exploring the uncertainty of κ_{chem} by taking κ_{gf} as the reference.

The results show that, although the slopes from linear fitting of κ_{chem} and κ_{gf} are close to 1.0, it is with quite poor ccorrelations (typically with correlation coefficients, R^2, of < 0.3) between κ_{chem} and κ_{gf} of the 80, 110, 150, 200 nm particles both in winter and summer. The poor correlations reflect large uncertainty in one or both of the calculated parameters that are likely due to the unreasonable assumption of particle mixing state (e.g. Cruz and Pandis, 2000; Svenningsson et al., 2006; Sjogren et al., 2007; Zardini et al., 2008), which varies with their aging and other physiochemical processes in the atmosphere. Note that underestimation of κ_{chem} for the summer occurred mostly in the afternoon (Marked in blue dots in Fig. 5). This may be associated with photochemical processes at around noontime. More specific investigations of the particle mixing and aging impacts on κ_{chem} will be further addressed in the following sections.

3.4 Aerosols aging processes and sources effects indicated by diurnal cycles of κ_{chem} and κ_{gf}

The diurnal cycles of particle hygroscopicity in the summer and winter with the use of the size-resolved chemical composition observations and the ratio of κ_{chem} to κ_{gf} are shown in Fig. 6. In summer, at 09:00-15:00, the disparity between κ_{chem} and κ_{gf} is insignificant for smaller particles (80 and 110 nm), both of which show slight decrease from 09:00 or 10:00 to 12:00-13:00 due to the frequent NPF event that usually corresponds to a large fraction of organics (Fig. 3) in urban Beijing. For larger particles (150 and 200 nm), the disparity between κ_{chem} and κ_{gf} around noontime and in the early afternoon is very significant, corresponding to >20% underestimation of particle hygroscopisity by κ_{chem} (with the ratio of κ_{chem} to κ_{gf} of ~0.8). Similar patterns were also noted by Zhang et al., (2017) but which is only based on a comparison between κ_{chem} derived from bulk chemical composition and κ_{gf}. Our results again indicate that the rapid photochemical aging of BC particles, which are generally with dominant size modes of 100-200 nm in the atmosphere, may lead to the core-shell structure in which certain secondary aerosol generated from photochemical reactions is thickly coated on the surface of BC (Wang et al., 2019). The hygroscopicity of the coated BC particles may only depend on the coating layer (Ma et al., 2013), thus resulting in the noontime/early afternoon underestimation of particle hygroscopicity by κ_{chem}. While, no significant differences between κ_{chem} and κ_{gf} are observed during night time. Note that κ_{chem} is slightly higher than κ_{gf} during early evening traffic rush hour and cooking time, when emissions of primary hydrophobic particles (e.g. BC and POA) are high (Fig. 3), thus resulting in a large percentage of externally-mixed particles). Causes of the overestimation in κ_{chem} during the traffic rush hour and cooking time will be discussed in the following paragraph. The particles experience rapid conversion and mixing in urban Beijing due to high precursor gases (Sun et al., 2015; Wu et al., 2016; Ren et al., 2018), and thus the coated/aged particles produced through photochemical processing in the afternoon can mix and interact with and freshly emitted primary particles emitted during rush hour (Wu et al., 2008). Therefore, during nighttime (22:00-06:00, LT), the particles are more uniform internally-mixed, which is reflective of the assumption for calculation of κ_{chem}, a much better consistency between κ_{chem} and κ_{gf} is observed.

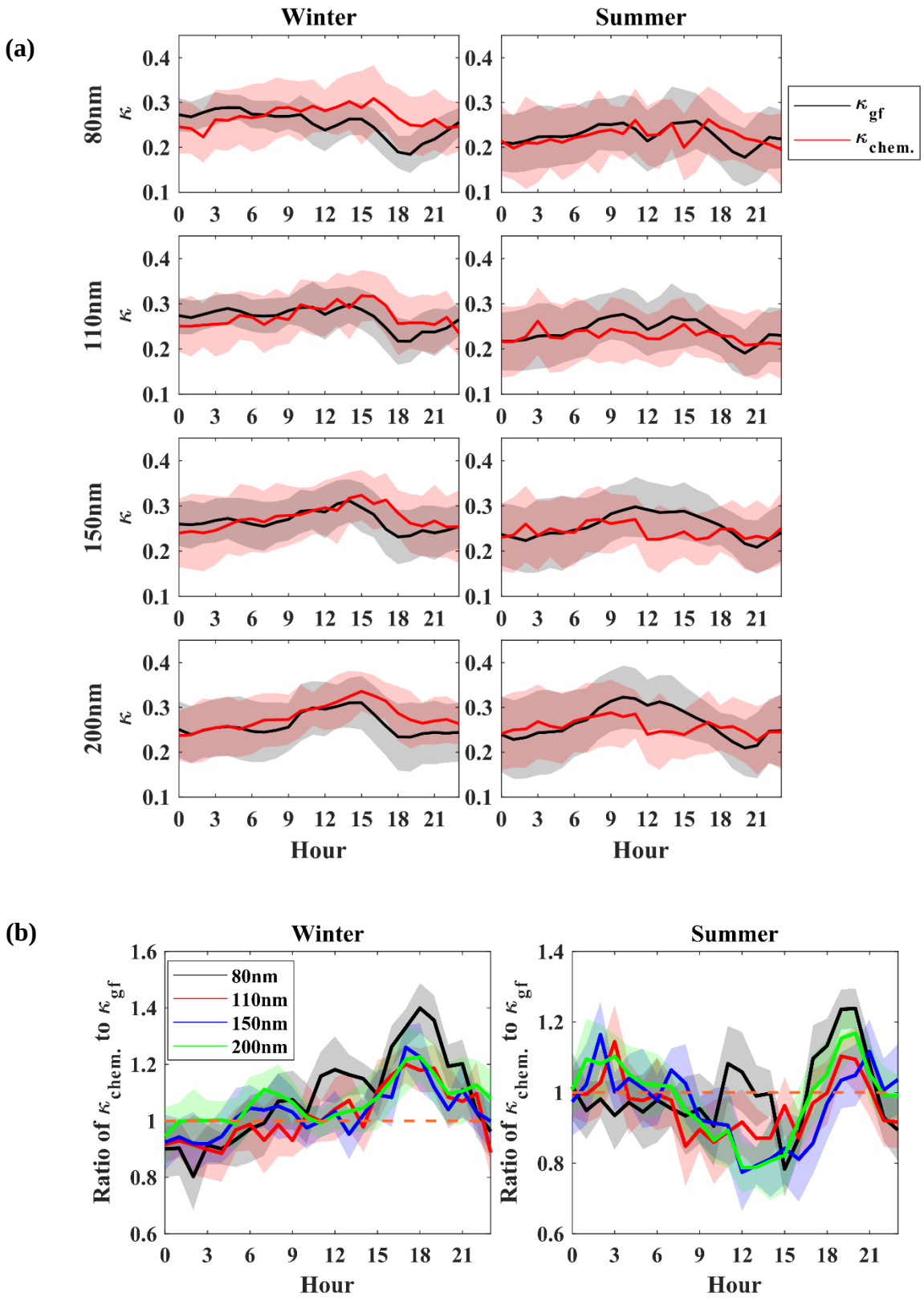

Figure 6. Diurnal variations of (a) κ_{chem} using size-resolved chemical composition data and κ_{gf} in winter and summer period; and (b) ratio of κ_{chem} to κ_{gf} in winter and summer period. The shade regions denote the error bars (1σ).

In winter, the disparity between κ_{chem} to κ_{gf} is insignificant at 09:00-15:00 due to the weakening effect of photochemical aging. From 15:00 to 21:00 LT, due to the strong vehicle and cooking sources around the site, the particles are dominated by the hydrophobic mode with a large concentration of externally-mixed BC and POA particles (Fig. 3), the calculated κ_{chem} is much higher than κ_{gf}, with the maximum ratio of κ_{chem} to κ_{gf} of 1.2-1.4, and the greatest disparity is observed for small particles. The disparity is further enhanced during clean periods when the hydrophobic mode is dominant (Fig. 7, Fig. S1).

We suppose that the large disparity between κ_{chem} and κ_{gf} is due to temporal variations in actual density of BC and organics caused by the particles aging and local sources. The externally-mixed BC particles are with fractal structure and chain-like aggregates and have been reported with effective density of 0.25-0.45 g cm^{-3}(McMurry et al., 2002), While the BC particles in the calculation is assumed as void free with effective density of 1.7 g cm^{-3}. Such inappropriate assumption would lead to an underestimation of BC volume fraction and thus the overestimation in κ_{chem} during the traffic rush hour and cooking time when BC particles are mostly freshly emitted with uncompacted structure. In addition, the significant increase in volume fraction of POA during the late afternoon would result in a lower density of organics, which is expected to be smaller than the assumed one (1.2 g cm^{-3}) in the calculation. A sensitivity test has been done to examine the effect of density of BC and organics on calculated κ_{chem} (Fig. 7). The result shows that the κ_{chem} value reduces by 16-33% when applying the BC effective density of 0.25-0.45 g cm^{-3}. This basically explains the disparity during the traffic rush hour. However, the changes in κ_{chem} are within $\pm$4% when changing the organic density from 1.0 (typical for POA) to 1.4 (typical for SOA) g cm^{-3}, suggesting insensitivity of κ_{chem} to variations of organic density. The result also indicates that, to fill the gap between κ_{chem} and κ_{gf} observed at noontime, the effective density of BC should be extremely high due to the decreased sensitivity of κ_{chem} to BC density with the aging of BC. In this case, the assumed density of BC is 1.7 g cm^{-3}, which reflects a very compacted and void free structure of the BC particles. The current applied value represents an upper limit for the effective density of ambient BC particles according to previous observations at a site near urban Beijing (Zhang et al., 2015), which suggested the aged BC is generally with effective density of 1.2 g cm^{-3}. Using this ambient observed density would lead to further underestimation in κ_{chem}. Our results exhibit the

increase of the density of BC and organics cannot explain the disparity between κ_{chem} and κ_{gf} observed around noontime in summer. This just, on the other hand, verifies the photochemical aging/coating effect on the aerosols hygroscopisity. In addition, the coexisting hygroscopic and hydrophobic species may have a strong influence on the phase state of particles, also likely affecting chemical interactions between inorganic and organic compounds as well as the overall hygroscopicity of mixed particles (Peng et al., 2016). Further investigations are needed to verify this. Our study suggest that, to accurately parameterize the effect of BC aging on particles hygroscopisty, future investigations need to measure the effective density and morphology of ambient BC, in particularity in those regions with complex local sources.

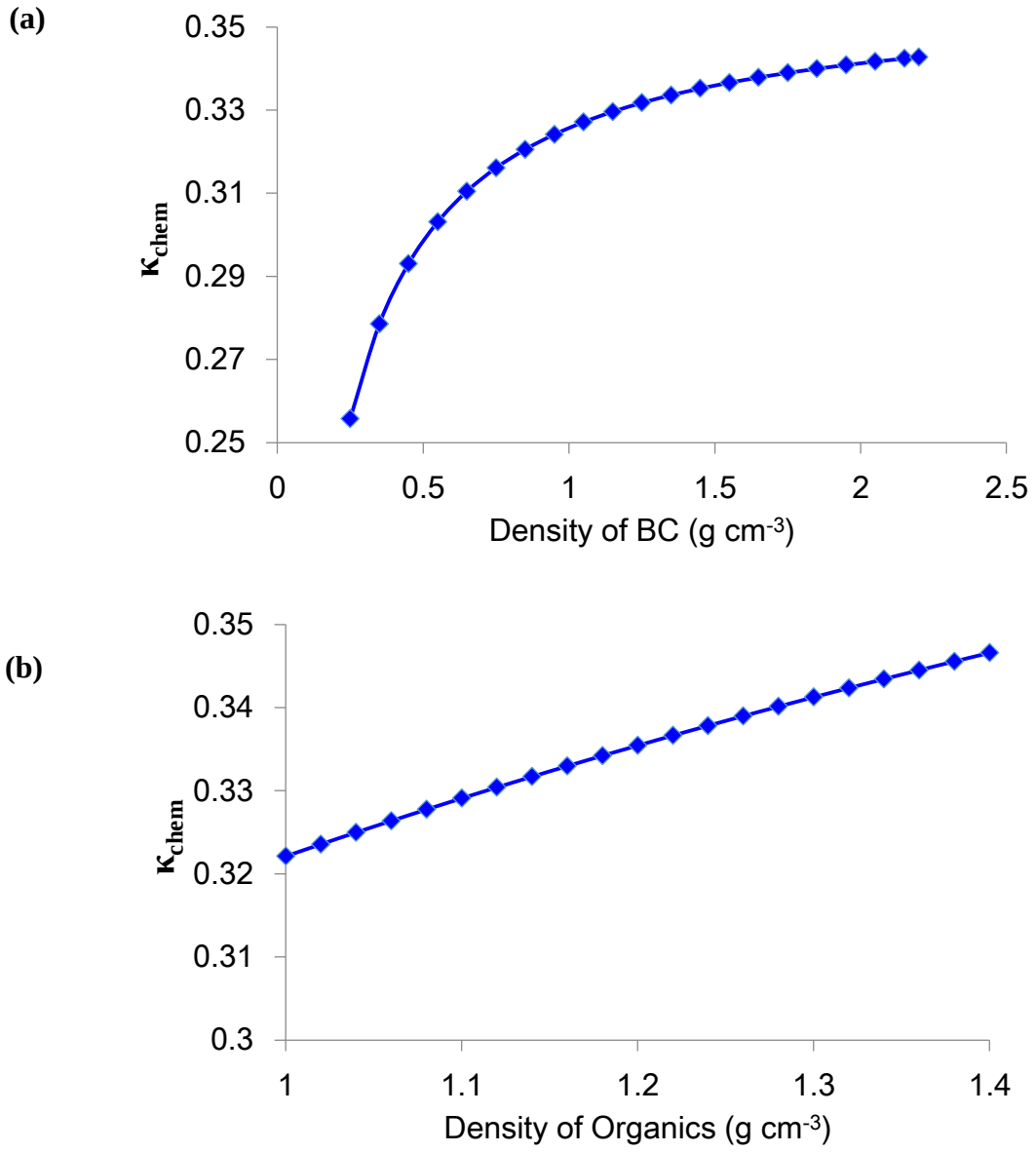

Figure 8. Sensitivity of κ_{chem} to variations of density of BC (a) and organics (b)

Besides the impacts of BC aging (changes in morphology/density) and variations of the overall density of organics on particles hygroscopicity, uncertainty in κ_{chem} may be related to the uncertainty in the hygroscopic parameter for organics that could vary widely over a range of diverse constitutes of SOA (Suda et al., 2012). However, Zhang et al. (2017) shown that using a smaller or larger κ_{SOA} could not fully explain the overestimation during traffic hours or the underestimation around noontime. Furthermore, in this study, it is calculated from a simple parametrized equation based on the AMS-measured f_{44} value reported by Mei et al. (2013). The value for f_{44} tends to be overestimated according to Fröhlich et al. (2015), which should yeild a larger κ_{chem}. Previous studies have shown that freshly emitted POA and BC particles may be rapidly coated by more hygroscopic components in polluted urban areas, resulting in enhanced hygroscopicity of the mixed particles (Zhang et al., 2004; Johnson et al., 2005; Zhao et al., 2017). Our results are consistent with those observations and clarify the photochemical aging and coating effect will largely underestimate the particles hygroscopicity using simple mixing rule based on chemical composition.

Note that during the nighttime, κ_{chem} is slight lower than κ_{gf}, with the minimum ratio of κ_{chem} to κ_{gf} of ~0.8 for 80 nm particles and ~0.9 for 110 and 150 nm particles at 02:00-04:00 LT (Fig. 6b), indicating an underestimation of particle hygroscopicity using composition data. The disparity at nighttime is further increased during heavily polluted events (Fig. S1), when the particles are more internally-mixed with only one hygroscopic mode (Fig. 8). We propose the increased underestimation during polluted conditions is likely due to enhanced condensation of secondary hygroscopic compounds (e.g. nitrate, sulfate) on pre-existing aerosols at lower temperature and higher relative humidity at nighttime (Wu et al., 2008; Wang et al., 2016; An et al., 2019). However, such condensation effect during nighttime is less significant (indicated by the smaller disparity between κ_{chem} and κ_{gf}) than the coating effect caused by aerosols photochemical aging at noontime, likely due to thinner coating layer formed on the pre-exist particles during nighttime or other factors influencing the particles hygroscopisity.

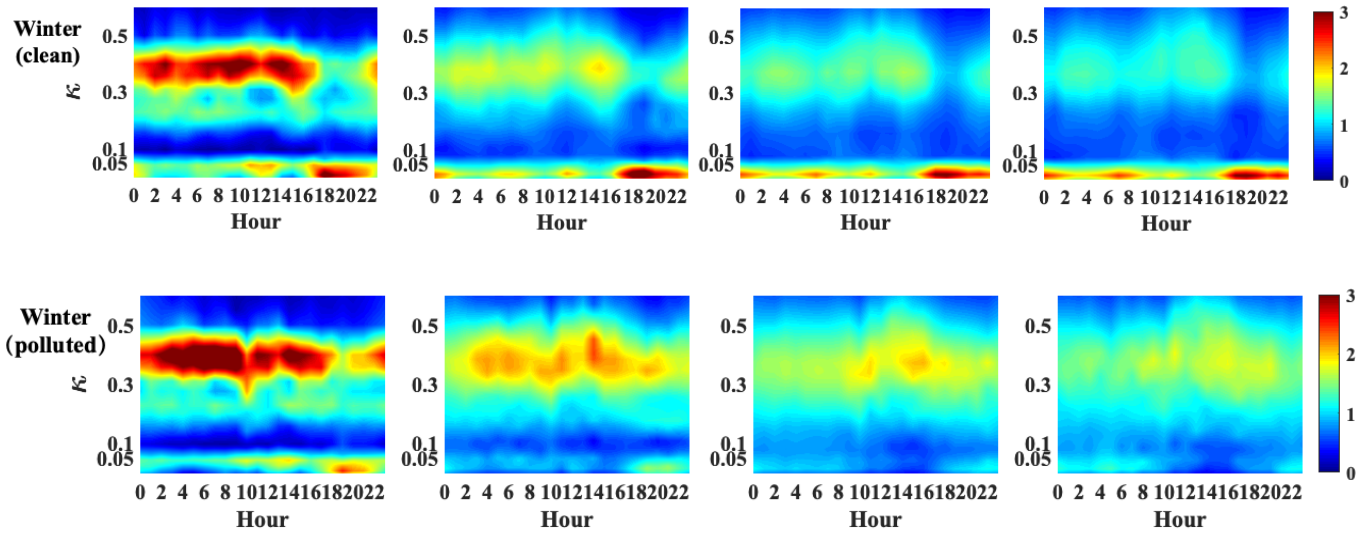

Figure 8. Diurnal cycles of κ_{gf} -PDF for 80, 110, 150 and 200 nm particles in clean and polluted events in winter.

3.5. Observation from other stations

The aging process in the summer period is related to photochemical processing in strong solar radiation conditions. The photochemical reactions produce sulfate and secondary organic aerosol, condensing on the surface of slightly- or non-hygroscopic primary aerosols (such as BC) (Zhang et al., 2008). As discussed in 3.4, the core-shell structure that accompanies aging of the particles results in calculated κ_{chem} that underestimates their hygroscopicity. To confirm such a coating effect on particle hygroscopicity, we further examine the diurnal variations of κ_{chem} and κ_{gf} or κ_{CCNc} (only at XZ site) based on observations in summer at two other sites in north China (Fig. 1). The XT site is located in the suburb of XT city, which is about 400 km south of Beijing, with high levels of industrialization and urbanization. Due to industrial emissions and typically weak ventilating winds, concentrations of $PM_{2.5,}$ black carbon and gaseous precursors are usually high at the site (Fu et al., 2014). Xinzhou is located in north of Taiyuan and about 360 km southwest of Beijing, and is surrounded by mountains on three sides. Local emissions from motor vehicles and industrial activities have relatively little influence on the sampled aerosol (Zhang et al., 2016). Because of its location and elevation, the aerosol at the XZ site is usually aged and transported from other areas. The sampling period was from July 22 to August 26, 2014 and from May 17 to June 14, 2016 at XZ and XT site respectively.

We find that the case at the XT site is very similar to that observed in BJ (Fig. 9a), with a lower κ_{chem} than κ_{gf} around noon time. But, because of much less influences from the local sources at XT compared to that at BJ, such underestimation by κ_{chem} continued until night at XT (Fig. 9b). Interestingly, a noontime lower κ_{chem} was not observed in the diurnal cycles at the XZ site, where κ_{chem} and κ_{CCNc} had similar diurnal patterns (Fig. 9c) with a roughly constant ratio of κ_{chem} to κ_{CCNc} of ~0.8-0.9 (Fig. 9d). This is probably because the XZ site is usually the recipient of aerosols transported from other areas that are already aged and well-mixed, with minimal impact of additional coating (Zhang et al., 2017). Also, the rate of oxidation and condensation may be slow in the relatively remote area where the gas precursors and oxidants are not as high as they are closer to sources regions. But at XT, which is located in the heavily polluted area in the north China Plain (Fu et al., 2014), aerosol emissions and processing are more similar to that in urban Beijing. These observations from other sites further confirms the the photochemical aging and coating effect that will largely underestimate the particles hygroscopicity using simple mixing rule based on chemical composition.

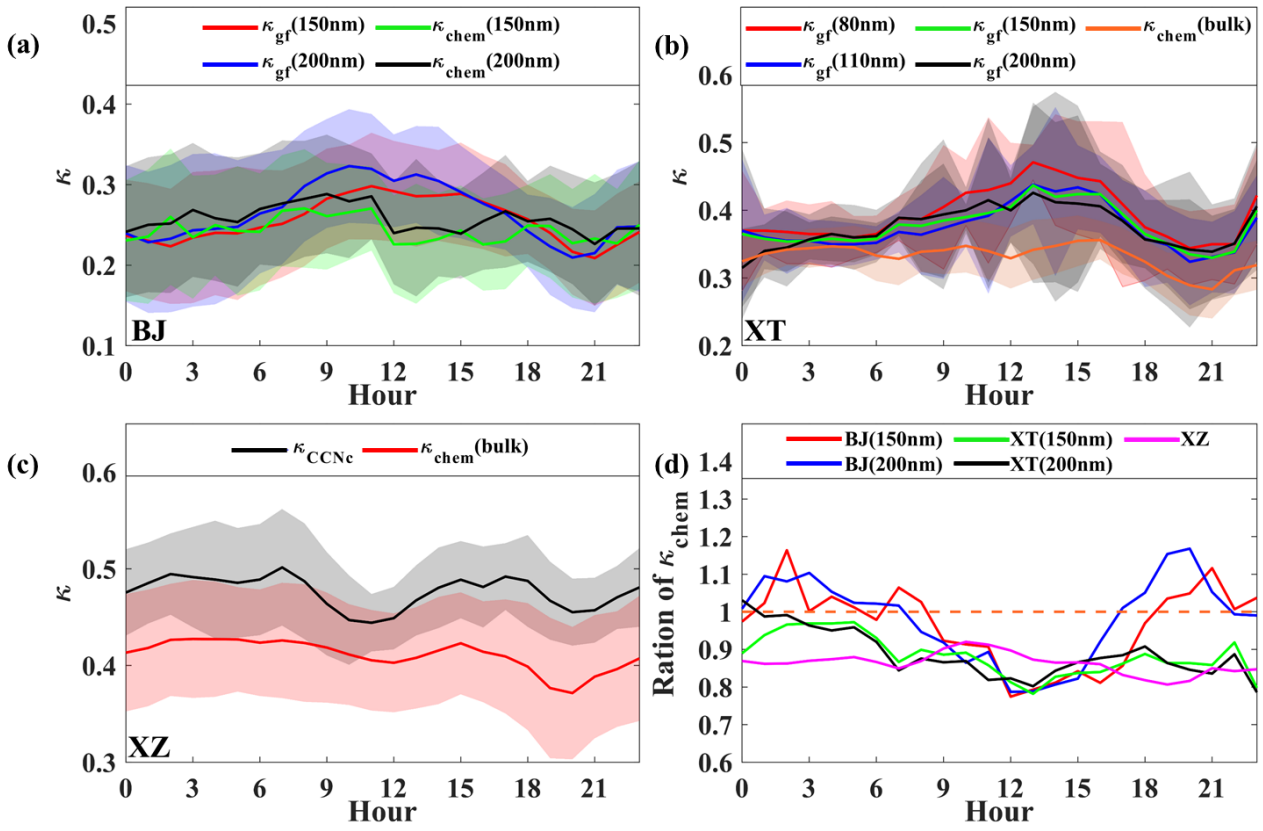

Figure 9. Diurnal variations in (a) κ_{chem} and κ_{gf} for 150 and 200 nm particles at BJ site; (b) κ_{chem} and κ_{gf} for 40, 80, 110, 150 and 200 nm particles at XT site; (c) κ_{chem} and mean κ_{CCNc} for particles at XZ site, and (d) ratio of mean κ_{chem} to κ_{gf} at the three sites.

4. Conclusion

Using measurements of aerosol composition and hygroscopicity made in Beijing (BJ) during a winter period of 2016 and a summer period of 2017, this paper analyzes the daily variation and seasonal differences of size-resolved aerosol hygroscopicity in urban Beijing. We mainly focus on studying the disparity of κ_{gf} and κ_{chem} between summer and winter to reveal the impact of atmospheric processes and mixing state of the particles on its hygroscopicity. The uncertainty in calculating κ by using chemical composition with a uniform internal mixing hypothesis is elucidated from the diurnal variations of the difference between the calculated values: in summer, lower κ_{chem} is obtained around noontime, with a ratio of κ_{chem} to κ_{gf} of about 0.8-0.9 for large particles (i.e. 150 nm and 200 nm), showing an underestimation of particles hygroscopisity by using simple mixing rule based on chemical composition. Combining with the observation from XT and XZ, we attribute the underestimation to the rapid noontime photochemical aging processes in summer, which induces the coating effect that will lead to a lower κ if assuming a uniform mixing of the particles. In contrast, larger κ_{chem} than κ_{gf} for >100 nm particles around noontime and in the early afternoon is derived in winter, with the maximum ratio of κ_{chem} to κ_{gf} of 1.2-1.4 when the particles are dominated by the hydrophobic mode with a large number of externally-mixed POA particles from strong vehicle and cooking sources. We attribute this large disparity between κ_{chem} and κ_{gf} to changes of BC morphology that can be indicated by effective density of BC. The sensitivity test shows that it can well explain the disparity during the traffic rush hour by applying BC effective density of 0.25-0.45 g cm^{-3}. However, we suggest that, to accurately parameterize or account for the effect of BC density on particles hygroscopisty, future investigations need to measure the effective density of ambient BC, in particularity in those regions with complex local sources.

A lower κ_{chem} than κ_{gf} for 80, 110 and 150 nm particles during the nighttime of winter is also noted, and the disparity is further enlarged in polluted days, probably due to a nighttime coating effect driven by

condensation of secondary hygroscopic species on pre-existing aerosols in cold season. Our results highlight the impacts of atmospheric processes, sources on aerosol mixing state and hygroscopicity, which should be quantified and considered in models for different atmospheric conditions.

Data availability. All data needed to evaluate the conclusions in the paper are present in the paper and/or the Supplementary Materials. Also, all data used in the study are available from the corresponding author upon request (fang.zhang@bnu.edu.cn).

Author contributions. F.Z. and J. L conceived the conceptual development of the manuscript. X. F. directed and performed of the experiments with L.C., X.J., Y. W., and F. Z.. F.Z., J.L., and X.F. conducted the data analysis and wrote the draft of the manuscript, and all authors edited and commented on the various sections of the manuscript. J.L. and X.F. contribute equally to this work.

Competing interests. The authors declare no competing interests.

Acknowledgements. This work was funded by National Natural Science Foundation of China (NSFC) research projects (grant nos. 41975174, 41675141, 91544217), the National Key R&D Program of China (grant no. 2017YFC1501702). We thank all participants of the field campaign for their tireless work and cooperation.

References

An, Z., Huang, R. J., Zhang, R., Tie, X., Li, G., Cao, J., Zhou, W., Shi, Z., Han, Y., Gu, Z., and Ji, Y.: Severe haze in Northern China: A synergy of anthropogenic emissions and atmospheric processes, Proceedings of the National Academy of Sciences, 116(18), 8657-8666, doi:10.1073/pnas.1900125116, 2019.

Bougiatioti, A., Fountoukis, C., Kalivitis, N., Pandis, S. N., Nenes, A., and Mihalopoulos, N.: Cloud condensation nuclei measurements in the marine boundary layer of the Eastern Mediterranean: CCN closure and droplet growth kinetics, Atmos. Chem. Phys., 9, 7053–7066, doi: 10.5194/acp-9-7053-2009, 2009.

Carrico, C. M., M. D. Petters, S. M. Kreidenweis, J. L. Collett Jr., G. Engling, and Malm W. C.: Aerosol hygroscopicity and cloud droplet activation of extracts of filters from biomass burning experiments, J. Geophys. Res., 113, D08206, doi:10.1029/2007JD009274. 2008.

Cerully, K. M., Raatikainen, T., Lance, S., Tkacik, D., Tiitta, P., Petäjä, T.,Nenes, A. : Aerosol hygroscopicity and CCN activation kinetics in a boreal forest environment during the 2007 EUCAARI campaign, Atmos. Chem. Phys., 11, 12369–12386, doi: 10.5194/acp-11-12369-2011, 2011.

Chang, R.-W., Liu, P., Leaitch, W., and Abbatt, J.: Comparison between measured and predicted CCN concentrations at Egbert, Ontario: Focus on the organic aerosol fraction at a semi-rural site, Atmos. Environ., 41, 8172–8182, 2007.

Collins, D. R., Flagan, R. C., and Seinfeld, J. H.: Improved inversion of scanning DMA data, Aerosol Sci. Technol., 36(1), 1–9, 2002.

Cruz, C. N. and Pandis, S. N.: Deliquescence and hygroscopic growth of mixed inorganic-organic atmospheric aerosol, Environ. Sci. Technol., 34, 4313–4319, doi: 10.1021/es9907109, 2000.

DeCarlo, P. F., Kimmel, J. R., Trimborn, A., Northway, M. J., Jayne, J. T., Aiken, A. C., Gonin, M., Fuhrer, K., Horvath, T., Docherty, K., Worsnop, D. R., and Jimenez, J. L.: Field-deployable, high-resolution, time-of-flight aerosol mass spectrometer, Anal. Chem., 78, 8281–8289, doi: 10.1021/ac061249n, 2006.

Fors, E. O., Swietlicki, E., Svenningsson, B., Kristensson, A.,Frank, G. P., and Sporre, M.: Hygroscopic properties of the ambient aerosol in southern Sweden – a two year study, Atmos. Chem. Phys., 11, 8343–8361, doi: 10.5194/acp-11-8343-2011, 2011.

Fröhlich, R., Crenn, V., Setyan, A., Belis, C. A., Canonaco, F., Favez, O., Riffault, V., Slowik, J. G., Aas, W., Aijälä, M., Alastuey, A., Artiñano, B., Bonnaire, N., Bozzetti, C., Bressi, M.,Carbone, C., Coz, E., Croteau, P. L., Cubison, M. J., Esser-Gietl,J. K., Green, D. C., Gros, V., Heikkinen, L., Herrmann, H., Jayne,J. T., Lunder, C. R., Minguillón, M. C., Mocnik, G., O'Dowd,C. D., Ovadnevaite, J., Petralia, E., Poulain, L., Priestman, M.,Ripoll, A., Sarda-Estève, R., Wiedensohler, A., Baltensperger,U., Sciare, J., and Prévôt, A. S. H.: ACTRIS ACSM intercomparison – Part 2: Intercomparison of ME-2 organic source apportionment results from 15 individual, co-located aerosol mass spectrometers, Atmos. Meas. Tech., 8, 2555–2576, doi:10.5194/amt-8-2555-2015, 2015.

Fu, G. Q., Xu, W. Y., Yang, R. F., Li, J. B., & Zhao, C. S. : The distribution and trends of fog and haze in the North China Plain over the past 30 years, Atmos. Chem. Phys., 14, 11949-11958, doi: 10.5194/acp-14-11949-2014, 2014.

Gasparini, R., R. Li, and D. R. Collins: Integration of size distributions and size-resolved hygroscopicity measured during the Houston Supersite for compositional categorization of the aerosol, Atmos. Environ., 38, 3285–3303, doi:10.1016/j.atmosenv.2004.03.019, 2004.

Good, N., Topping, D. O., Allan, J. D., Flynn, M., Fuentes, E.,Irwin, M., Williams, P. I., Coe, H., and McFiggans, G.: Consistency between parameterisations of aerosol hygroscopicity and CCN activity during the RHaMBLe discovery cruise, Atmos. Chem. Phys., 10, 3189–3203, doi: 10.5194/acp-10-3189-2010, 2010.

Gunthe, S. S., King, S. M., Rose, D., Chen, Q., Roldin, P., Farmer,D. K., Jimenez, J. L., Artaxo, P., Andreae, M. O., Martin, S.T., and Pöschl, U.: Cloud condensation nuclei in pristine tropical rainforest air of Amazonia: size-resolved measurements and modeling of atmospheric aerosol composition and CCN activity, Atmos. Chem. Phys., 9, 7551–7575, doi: 10.5194/acp-9-7551-2009, 2009.

Gysel, M., Crosier, J., Topping, D. O., Whitehead, J. D., Bower, K.N., Cubison, M. J., Williams, P. I., Flynn, M. J., McFiggans, G.B., and Coe, H.: Closure study between chemical composition and hygroscopic growth of aerosol particles during TORCH2, Atmos. Chem. Phys., 7, 6131–6144, doi: 10.5194/acp-7-6131-2007, 2007.

Gysel, M., McFiggans, G. B., and Coe, H.: Inversion of tandem differential mobility analyser (TDMA) measurements, J. Aerosol Sci., 40, 134–151, doi: 10.1016/j.jaerosci.2008.07.013, 2009.

Hu, W., Hu, M., Hu, W., Jimenez, J. L., Yuan, B., Chen, W., Wang, M., Wu, Y., Chen, C., Wang, Z., Peng, J., Zeng, L., and Shao, M.: Chemical composition, sources, and aging process of submicron aerosols in Beijing: Contrast between summer and winter, J. Geophys. Res., 121, 1955–1977, doi: 10.1002/2015JD024020, 2016.

Irwin, M., Good, N., Crosier, J., Choularton, T. W., & McFiggans, G.: Reconciliation of measurements of hygroscopic growth and critical supersaturation of aerosol particles in central Germany Atmos. Chem. Phys., 10, 11737–11752, doi:10.5194/acp-10-11737-2010, 2010.

513 Jacobson, M.Z. : Strong radiative heating due to the mixing state of black carbon in atmospheric aerosols,
514 Nature, 409(6821):695-697, 2001.
515 Johnson, K. S., Zuberi, B., Molina, L. T., Molina, M. J., Iedema, M. J., Cowin, J. P., Gaspar, D. J., Wang, C.,
516 and Laskin, A.: Processing of soot in an urban environment: Case study from the Mexico City
517 Metropolitan Area, Atmos. Chem. Phys.,5, 3033–3043, doi: 10.5194/acp-5-3033-2005, 2005.
518 Kulmala, M., Petaja, T., Monkkonen, P., Koponen, I.K., Dal Maso, M.,Aalto, P.P., Lehtinen, K.E.J., and
519 Kerminen, V.M. : On the growth of nucleation mode particles: source rates of condensable vapor in
520 polluted and clean environments, Atmos. Chem. Phys., 5, 409–416, doi: 10.5194/acp-5-409-2005, 2005.
521 Kuwata, M., Kondo, Y., Miyazaki, Y., Komazaki, Y., Kim, J. H.,Yum, S. S., Tanimoto, H., and Matsuedda,
522 H.: Cloud condensation nuclei activity at Jeju Island, Korea in spring 2005, Atmos. Chem. Phys., 8,
523 2933–2948,doi:10.5194/acp-8-2933-2008,2008.
524 Liu, D., Joshi, R., Wang, J., Yu, C., Allan, J. D., Coe, H., Flynn, M. J., Xie, C., Lee, J., Squires, F., Kotthaus,
525 S., Grimmond, S., Ge, X., Sun, Y., and Fu, P.: Contrasting physical properties of black carbon in urban
526 Beijing between winter and summer, Atmos. Chem. Phys. Discuss., doi: 10.5194/acp-2018-1142, in
527 review, 2018.
528 Liu, P. F., Zhao, C. S., Göbel, T., Hallbauer, E., Nowak, A., Ran,L., Xu, W. Y., Deng, Z. Z., Ma, N.,
529 Mildenberger, K., Henning,S., Stratmann, F., and Wiedensohler, A.: Hygroscopic properties of aerosol
530 particles at high relative humidity and their diurnal variations in the North China Plain, Atmos. Chem.
531 Phys., 3479–3494, doi:10.5194/acp-11-3479-2011, 2011.
532 Ma, Y., Brooks, S. D., Vidaurre, G., Khalizov, A. F., Wang, L., and Zhang, R.: Rapid modification of
533 cloud-nucleating ability of aerosols by biogenic emissions, Geophys. Res. Lett., 40, 6293–6297, doi:
534 10.1002/2013GL057895, 2013.
535 Massling, A., Stock, M., and Wiedensohler, A.: Diurnal, weekly, and seasonal variation of hygroscopic
536 properties of submicrometer urban aerosol particles, Atmos. Environ., 39(21), 3911–3922, doi:
537 10.1016/j.atmosenv.2005.03.020, 2005.
538 McMurry, P. H.; Wang, X.; Park, K.; Ehara, K. The Relationship between Mass and Mobility for
539 Atmospheric Particles. Aerosol Sci. Technol., 36, 227-238, 2002.

Mei, F., Hayes, P. L., Ortega, A. M., Taylor, J. W., Allan, J. D., Gilman, J. B., Kuster, W. C., de Gouw, J. A., Jimenez, J. L., and Wang, J.: Droplet activation properties of organic aerosols observed at an urban site during CalNex-LA, J. Geophys. Res., 118, 2903–2917, doi: 10.1002/jgrd.50285, 2013.

Mikhailov, E. F., Mironov, G. N., Pöhlker, C., Chi, X., Krüger, M. L., Shiraiwa, M., Förster, J. D., Pöschl, U., Vlasenko, S. S., Ryshkevich, T. I., Weigand, M., Kilcoyne, A. L. D., and Andreae, M. O.: Chemical composition, microstructure, and hygroscopic properties of aerosol particles at the Zotino Tall Tower Observatory (ZOTTO), Siberia, during a summer campaign, At-mos. Chem. Phys., 15, 8847–8869, doi:10.5194/acp-15-8847-2015, 2015.

Peng, C., Jing, B., Guo, Y. C., Zhang, Y. H., and Ge, M. F.: Hygroscopic behavior of multicomponent aerosols involving nacl and dicarboxylic acids. J. Phys. Chemis. A, 120(7), 1029-1038, 2016.

Peng, J., Hu, M., Guo, S., Du, Z., Shang, D., and Zheng, J.: Ageing and hygroscopicity variation of black carbon particles in beijing measured by a quasi-atmospheric aerosol evolution study (quality) chamber. Atmospheric Chemistry and Physics, 17(17), 10333-10348, 2017.

Petters, M. D. and Kreidenweis, S. M.: A single parameter representation of hygroscopic growth and cloud condensation nucleus activity, Atmos. Chem. Phys., 7, 1961–1971, doi: 10.5194/acp-7-1961-2007, 2007.

Ren, J. Y., Zhang, F., Wang, Y. Y., Collins, D., Fan, X. X., Jin, X. A., Xu, W. Q., Sun, Y. L., Cribb, M., and Li, Z. Q.: Using different assumptions of aerosol mixing state and chemical composition to predict CCN concentrations based on field measurements in urban Beijing, Atmos. Chem. Phys., 18, 6907–6921, doi: 10.5194/acp-18-6907-2018, 2018.

Rose, D., Nowak, A., Achtert, P., Wiedensohler, A., Hu, M., Shao, M., Zhang, Y., Andreae, M. O., and Pöschl, U.: Cloud condensation nuclei in polluted air and biomass burning smoke near the mega-city Guangzhou, China – Part 1: Size-resolved measurements and implications for the modeling of aerosol particle hygroscopicity and CCN activity, Atmos. Chem. Phys.,10, 3365–3383, https://doi.org/10.5194/acp-10-3365-2010, 2010.

Saarnio, K., Frey, A., Niemi, J. V., Timonen, H., Rönkkö, T., Karjalainen, P., Vestenius, M., Teinilä, K., Pirjola, L., Niemelä, V.,Keskinen, J., Häyrinen, A., and Hillamo, R.: Chemical composition and size of

566 particles in emissions of coal-fired power plant with flue gas desulphurization, J. Aerosol Sci., 73, 14–26,
567 2014.
568 Schill, S. R., Collins, D. B., Lee, C., Morris, H. S., Novak, G. A., and Prather, K. A.: The impact of aerosol
569 particle mixing state on the hygroscopicity of sea spray aerosol. ACS Central Science, 1(3), 132-141,
570 2015
571 Sjogren, S., Gysel, M., Weingartner, E., Baltensperger, U., Cubison,M. J., Coe, H., Zardini, A. A., Marcolli,
572 C., Krieger, U. K., and Peter, T.: Hygroscopic growth and water uptake kinetics of two-phase aerosol
573 particles consisting of ammonium sulfate, adipic and humic acid mixtures, J. Aerosol Sci., 38, 157–171,
574 doi: 10.1016/j.jaerosci.2006.11.005, 2007.
575 Suda, S. R., Petters, M. D., Matsunaga, A., Sullivan, R. C., Ziemann, P. J., and Kreidenweis, S. M.:
576 Hygroscopicity frequency distributions of secondary organic aerosols. J.Geophys. Res., 117(D4), D04207,
577 2012
578 Svenningsson, B., Rissler, J., Swietlicki, E., Mircea, M., Bilde, M.,Facchini, M. C., Decesari, S., Fuzzi, S.,
579 Zhou, J., Mønster, J., and Rosenørn, T.: Hygroscopic growth and critical supersaturations for mixed
580 aerosol particles of inorganic and organic compounds of atmospheric relevance, Atmos. Chem. Phys., 6,
581 1937–1952, doi:10.5194/acp-6-1937-2006, 2006.
582 Sun, Y. L., Wang, Z. F., Du, W., Zhang, Q., Wang, Q. Q., Fu, P. Q., Pan, X. L., Li, J., Jayne, J., and
583 Worsnop, D. R.: Long-term real-time measurements of aerosol particle composition in Beijing, China:
584 Seasonal variations, meteorological effects, and source analysis, Atmos. Chem. Phys., 15, 10149–10165,
585 doi: 10.5194/acp-15-10149-2015, 2015.
586 Sun, Y., Du, W., Fu, P., Wang, Q., Li, J., Ge, X., Zhang, Q., Zhu, C., Ren, L., Xu, W., Zhao, J., Han, T.,
587 Worsnop, D. R., and Wang, Z.: Primary and secondary aerosols in Beijing in winter: sources, variations
588 and processes, Atmos. Chem. Phys., 16, 8309–8329, doi: 10.5194/acp-16-8309-2016, 2016.
589 Swietlicki, E., Hansson, H. C., HÄMeri, K., Svenningsson, B., Massling, A., McFiggans, G., McCurry, P.
590 H., PetÄJÄ, T., Tunved, P., Gysel, M., Topping, D., Weingartner, E., Bal-tensperger, U., Rissler, J.,
591 Wiedensohler, A., and Kulmala, M.: Hygroscopic properties of submicrometer atmospheric aerosol

592 particles measured with H-TDMA instruments in various environments - a review, Tellus B, 60, 432–469,
593 doi: 10.1111/j.1600-0889.2008.00350.x, 2008.
594 Tan, H., Xu, H., Wan, Q., Li, F., Deng, X., Chan, P. W., Xia, D., and Yin, Y.: Design and application of an
595 unattended multifunctional H-TDMA system, J. Atmos. Ocean. Tech., 30, 1136–1148, doi:
596 10.1175/JTECH-D-12-00129.1, 2013.
597 Turpin, B. J. and Lim, H. J.: Species contributions to PM2.5 mass concentrations: Revisiting common
598 assumptions for estimating organic mass, Aerosol Sci. Tech., 35, 602–610, doi:
599 10.1080/02786820152051454, 2001.
600 Wang, J., Cubison, M. J., Aiken, A. C., Jimenez, J. L., and Collins, D. R.: The importance of aerosol mixing
601 state and size-resolved composition on CCN concentration and the variation of the importance with
602 atmospheric aging of aerosols, Atmos. Chem. Phys., 10, 7267–7283, doi:10.5194/acp-10-7267-2010,
603 2010.
604 Wang, J., Zhang, Q., Chen, M.-D., Collier, S., Zhou, S., Ge, X., Xu, J., Shi, J., Xie, C., Hu, J., Ge, S., Sun,
605 Y., and Coe, H.: First chemical characterization of refractory black carbon aerosols and associated
606 coatings over the Tibetan Plateau (4730 m a.s.l), Environ. Sci. Tech., 51, 14072,
607 doi:10.1021/acs.est.7b03973, 2017.
608 Wang, J. F., Liu, D. T., Ge, X. L., Wu, Y. Z., Shen, F. Z., Chen, M. D., Zhao, J., Xie, C. H., Wang, Q. Q.,
609 Xu, W. Q., Zhang, J., Hu, J. L., Allan, J., Joshi, R., Fu, P. Q., Coe, H., and Sun, Y. L.: Characterization of
610 black carbon-containing fine 10 particles in Beijing during wintertime, Atmos. Chem. Phys., 19, 447-458,
611 doi: 10.5194/acp-19-447-2019, 2019.
612 Wang, Q., Zhao, J., Du, W., Ana, G., Wang, Z., Sun, L., Wang, Y., Zhang, F., Li, Z., Ye, X., and Sun, Y.:
613 Characterization of submicron aerosols at a suburban site in central China, Atmos. Environ., 131, 115–
614 123, doi:10.1016/j.atmosenv.2016.01.054, 2016.
615 Wang, S. C. and Flagan, R. C.: Scanning Electrical Mobility Spectrometer, Aerosol Sci. Tech., 13, 230–240,
616 1990.

Wang, Y., Zhang, F., Li, Z., Tan, H., Xu, H., Ren, J., Zhao, J., Du, W., and Sun, Y.: Enhanced hydrophobicity and volatility of submicron aerosols under severe emission control conditions in Beijing, Atmos. Chem. Phys., 17, 5239–5251, doi: 10.5194/acp-17-5239-2017, 2017.

Wang Y., Li Z., Zhang Y., Du W., Zhang F., Tan H., Xu H., Fan T., Jin X., Fan X., Dong Z., Wang Q. and Sun Y.: Characterization of aerosol hygroscopicity, mixing state, and CCN activity at a suburban site in the central North China Plain, Atmos. Chem. Phys., 18, 11739-11752, doi: 10.5194/acp-18-11739-2018, 2018a.

Wang, Y., Z. Wu, N. Ma, Y. Wu, L. Zeng, C. Zhao, and A. Wiedensohler: Statistical analysis and parameterization of the hygroscopic growth of the sub-micrometer urban background aerosol in Beijing, Atmos. Environ., 175, 184-191, doi: 10.1016/j.atmosenv.2017.12.003, 2018b.

Wex, H., Petters, M. D., Carrico, C. M., Hallbauer, E., Massling,A., McMeeking, G. R., Poulain, L., Wu, Z., Kreidenweis, S. M.,and Stratmann, F. :Towards closing the gap between hygroscopic growth and activation for secondary organic aerosol: Part 1—Evidence from measurements, Atmos. Chem. Phys., 9, 3987–3997, doi: 10.5194/acp-9-3987-2009, 2009

Wu, Z., Hu, M., Lin, P., Liu, S., Wehner, B., and Wiedensohler, A.: Particle number size distribution in the urban atmosphere of Beijing, China, Atmos. Environ., 42, 7967–7980, doi: 10.1016/j.atmosenv.2008.06.022, 2008.

Wu, Z. J., Poulain, L., Henning, S., Dieckmann, K., Birmili, W.,Merkel, M., van Pinxteren, D., Spindler, G., Müller, K., Strat-mann, F., Herrmann, H., and Wiedensohler, A.: Relating particle hygroscopicity and CCN activity to chemical composition during the HCCT-2010field campaign, Atmos. Chem. Phys., 13, 7983–7996, doi: 10.5194/acp-13-7983-2013, 2013.

Wu, Z. J., Zheng, J., Shang, D. J., Du, Z. F., Wu, Y. S., Zeng, L. M., Wiedensohler, A., and Hu, M.: Particle hygroscopicity and its link to chemical composition in the urban atmosphere of Beijing, China, during summertime, Atmos. Chem. Phys., 16, 1123–1138, doi: 10.5194/acp-16-1123-2016, 2016.

Xu, W. Q., Sun, Y. L., Chen, C., Du, W., Han, T. T., Wang, Q. Q.,Fu, P. Q., Wang, Z. F., Zhao, X. J., Zhou, L. B., Ji, D. S., Wang,P. C., and Worsnop, D. R.: Aerosol composition, oxidation properties, and sources

in Beijing: results from the 2014 Asia-Pacific Economic Cooperation summit study, Atmos. Chem. Phys., 15,13681–13698, doi:10.5194/acp-15-13681-2015, 2015.

Ye, X., Tang, C., Yin, Z., Chen, J., Ma, Z., Kong, L., Yang, X., Gao, W., and Geng, F.: Hygroscopic growth of urban aerosol particles during the 2009 Mirage-Shanghai Campaign, Atmos. Environ., 64, 263–269, doi:10.1016/j.atmosenv.2012.09.064, 2013.

Zardini, A. A., Sjogren, S., Marcolli, C., Krieger, U. K., Gysel,M., Weingartner, E., Baltensperger, U., and Peter, T.: A combined particle trap/HTDMA hygroscopicity study of mixed in-organic/organic aerosol particles, Atmos. Chem. Phys., 8, 5589–5601, doi:10.5194/acp-8-5589-2008, 2008

Zhang, F., Li, Y., Li, Z., Sun, L., Li, R., Zhao, C., Wang, P., Sun, Y., Liu, X., Li, J., Li, P., Ren, G., and Fan, T.: Aerosol hygroscopicity and cloud condensation nuclei activity during the AC3Exp campaign: Implications for cloud condensation nuclei parameterization, Atmos. Chem. Phys., 14, 13423–13437, doi: 10.5194/acp-14-13423-2014, 2014.

Zhang, F., Li, Z., Li, Y., Sun, Y., Wang, Z., Li, P., Sun, L., Wang, P., Cribb, M., Zhao, C., Fan, T., Yang, X., and Wang, Q.: Impacts of organic aerosols and its oxidation level on CCN activity from measurement at a suburban site in China, Atmos. Chem. Phys., 16, 5413–5425, doi: 10.5194/acp-16-5413-2016, 2016.

Zhang, F., Wang, Y., Peng, J., Ren, J., Zhang, R., Sun, Y., Collin, D., Yang, X., and Li, Z.: Uncertainty in predicting CCN activity of aged and primary aerosols, J. Geophys. Res.-Atmos., 122, 11723–11736, doi: 10.1002/2017JD027058, 2017.

Zhang, R., Khalizov, A. F., Pagels, J., Zhang, D., Xue, H., and McMurry, P. H.: Variability in morphology, hygroscopicity, and op-tical properties of soot aerosols during atmospheric processing, PNAS, 105(30), 10291–10296, doi:10.1073/pnas.0804860105, 2008.

Zhang, R., Wang, G., Guo, S. Zamora, M. and Wang. Y.: Formation of urban fine particulate matter. Chemical Reviews, 115(10), 3803-3855, 2015

Zhang, Q., Stanier, C. O., Canagaratna, M. R., Jayne, J. T., Worsnop, D. R., Pandis, S. N., & Jimenez, J. L. : Insights into the chemistry of new particle formation and growth events in Pittsburgh based on aerosol mass spectrometry, Environ. Sci. Tech., 38(18), 4797–4809, doi: 10.1021/es035417u, 2004.

Zhang, Y., Zhang, Q., Cheng, Y., Su, H., Kecorius, S., Wang, Z., Wu, Z., Hu, M., Zhu, T., Wiedensohler, A.,

and He, K.: Measuring the morphology and density of internally mixed black carbon with SP2 and VTDMA: new insight into the absorption enhancement of black carbon in the atmosphere, Atmos. Meas. Tech., 9, 1833-1843, 2016.

Zhao, J., Du, W., Zhang, Y., Wang, Q., Chen, C., Xu, W., Han, T., Wang, Y., Fu, P., Wang, Z., Li, Z., and Sun, Y.: Insights into aerosol chemistry during the 2015 China Victory Day parade: results from simultaneous measurements at ground level and 260 m in Beijing, Atmos. Chem. Phys., 17, 3215–3232, doi: 10.5194/acp-17-3215-2017, 2017.